Science Advances
AAAS

advances.sciencemag.org/cgi/content/full/6/15/eaaz4322/DC1

# Supplementary Materials for

## Exploiting equilibrium-kinetic synergetic effect for separation of ethylene and ethane in a microporous metal-organic framework

Qi Ding, Zhaoqiang Zhang, Cong Yu, Peixin Zhang, Jun Wang, Xili Cui, Chao-Hong He, Shuguang Deng, Huabin Xing*

*Corresponding author. Email: xinghb@zju.edu.cn

Published 10 April 2020, *Sci. Adv.* **6**, eaaz4322 (2020)
DOI: 10.1126/sciadv.aaz4322

**This PDF file includes:**

**Equilibrium adsorption measurement**

The adsorption isotherms of ethylene and ethane on $ZnAtzPO_4$ were analyzed on the instrument of Micromeritics ASAP 2460. Before each measurement, about 100 mg of $ZnAtzPO_4$ material was loaded into glass analysis tube and heated at 100℃ for 12 h under high vacuum (< 7 μmHg). The sample was backfilled with $N_2$ before transferred to the analysis port, where it was evacuated for another 120 minutes before the analysis started. The equilibrium interval (i.e., the time during which the pressure must remain stable within a small range) was set as 10 s, except that for $C_2H_6$ at 273 K and 288 K was prolonged to 20 s due to the slow diffusion under low-temperature environment.

**Calculation of isosteric heat of adsorption**

The isosteric heat of adsorption profiles for $C_2H_4$ and $C_2H_6$ were derived from adsorption isotherms measured at 273 K, 288 K and 298 K by Virial fitting method and Clausius-Claperyron equation.

A Virial-type expression was used (eq. 1), where $p$ represents the pressure in mmHg, $n$ represents the gas uptake in mg $g^{-1}$, $T$ represents the temperature in Kelvin, $a_i$ and $b_i$ are Virial coefficients independent of temperature, $c$ and $d$ are the numbers of coefficients required to adequately describe the isotherms.

$$\ln p = \ln n + \frac{1}{T}\sum_{i=0}^{c} a_i n^i + \sum_{j=0}^{d} b_j n^j \qquad (1)$$

$$K_H = \exp(-b_0) \times \exp(\frac{-a_0}{T}) \qquad (2)$$

The isosteric heat of adsorption ($Q_{st}$) is calculated according to the following equation derived from the Clausius-Claperyron equation (eq. 3).

$$Q_{st} = -R\left[\frac{\partial \ln p}{\partial\left(\frac{1}{T}\right)}\right]_n = -R\sum_{i=0}^{m} a_i n^i \qquad (3)$$

**Density functional theory calculations**

DFT-D calculations were performed with CASTEP code (Segal *et al*. *J. Phys. Condens. Matter* **2002**, 14, 2717) implemented in the Materials Studio software. A semi-empirical addition of dispersive forces to conventional DFT was included in the calculation to account for van der Waals interactions. Calculations were performed under the generalized gradient approximation (GGA) with Perdew-Burke-Ernzerhof (PBE) exchange correlation. A cutoff energy of 544 eV and a 2 × 2 × 2 k-point mesh were found to be enough for the total energy to converge within $1 \times 10^{-5}$ eV $atom^{-1}$. We first optimized the structure of $ZnAtzPO_4$, which agrees well with the reported $ZnAtzPO_4$ (guest-free) structure. $C_2H_4$/$C_2H_6$ gas molecules were then introduced to various locations of the channel pore, followed by a full structural relaxation.

**Molecular dynamic simulations**

The molecular dynamic (MD) simulations were performed in the Forcite module of Material Studio. The initial configurations used for MD simulations were taken from DFT calculations. The simulation box contains eight unit cells. The constant-volume & temperature (NVT) ensemble was used. The Lennard-Jones (L-J) parameters from the DREIDING force field (Mayo *et al*. *J. Phys. Chem.* **1990**, 94, 8897), and atomic charges from previous report (Vaidhyanathan *et al*. *Angew. Chem. Int. Ed.* **2012**, 51, 1826) were directly employed to the current work. The cutoff radius was chosen as 15.5 Å for the LJ potential. The electrostatic interactions and the van der Waals interactions were evaluated by the Ewald summation method,

with a Buffer width of 0.5 Å. The time step and total simulation time were set as 1.0 fs and 5.0 ns, respectively. The first 3 ns were used as equilibrium and the following 2 ns were adopted for analysis of diffusion behaviors. The temperature was 298 K.

**Breakthrough experiment**

The breakthrough experiments were conducted on a dynamic gas breakthrough equipment (Cui *et al*. *Science* **2016**, 353, 141). In a typical procedure, a stainless-steel column (Φ 4.6 × 50 mm) packed with 0.82 g of $ZnAtzPO_4$ material was firstly activated by purge with a flow of He gas (10 mL/min) at 100℃ for 12 h. A gas mixture of ethene/ethane (50:50, v/v) was then introduced into the column at a rate of 0.75 mL/min under 273 K and 1 bar. The concentration of the gas eluted from the outlet was detected by chromatography (GC-490) with the thermal conducticity detector TCD. After the breakthrough experiment, the column was regenerated by purge with He, at 100℃ for 12 h.

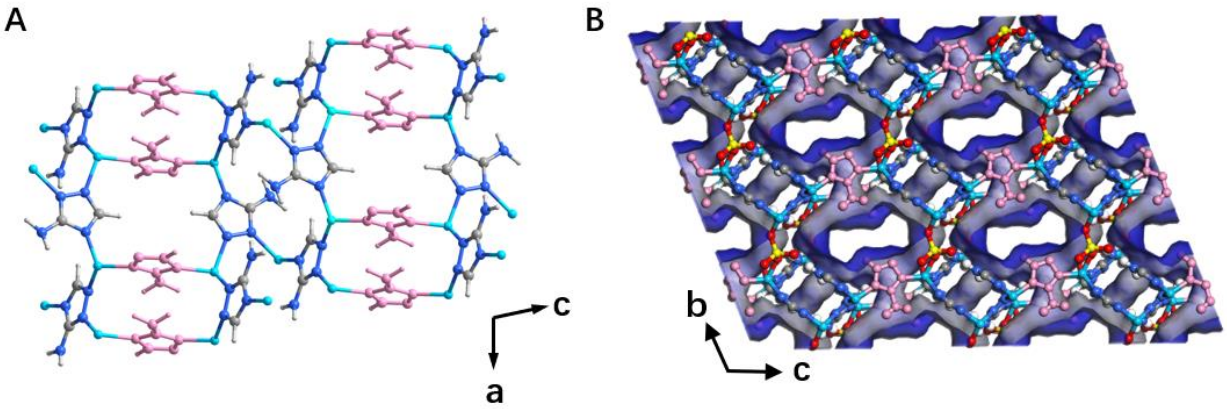


**Figure S1.** Schematic illustration of the structure of $ZnAtzPO_4$. (A) Structure of the two-dimensional cationic layer consisting of deprotonated Atz ligands and $Zn^{2+}$ cations. (B) Connolly surface (Connolly radius = 1.0 Å) showing the three-dimensional structure of $ZnAtzPO_4$ and the channel decorated by

intruding amino groups from the ligands and oxygen atoms from the anion pillars. (Color mode: C, gray-40%; H, white; N, light blue; Zn, sky blue; P, yellow; O, red. Bidentate coordinated Atz ligands are highlighted by rose.)

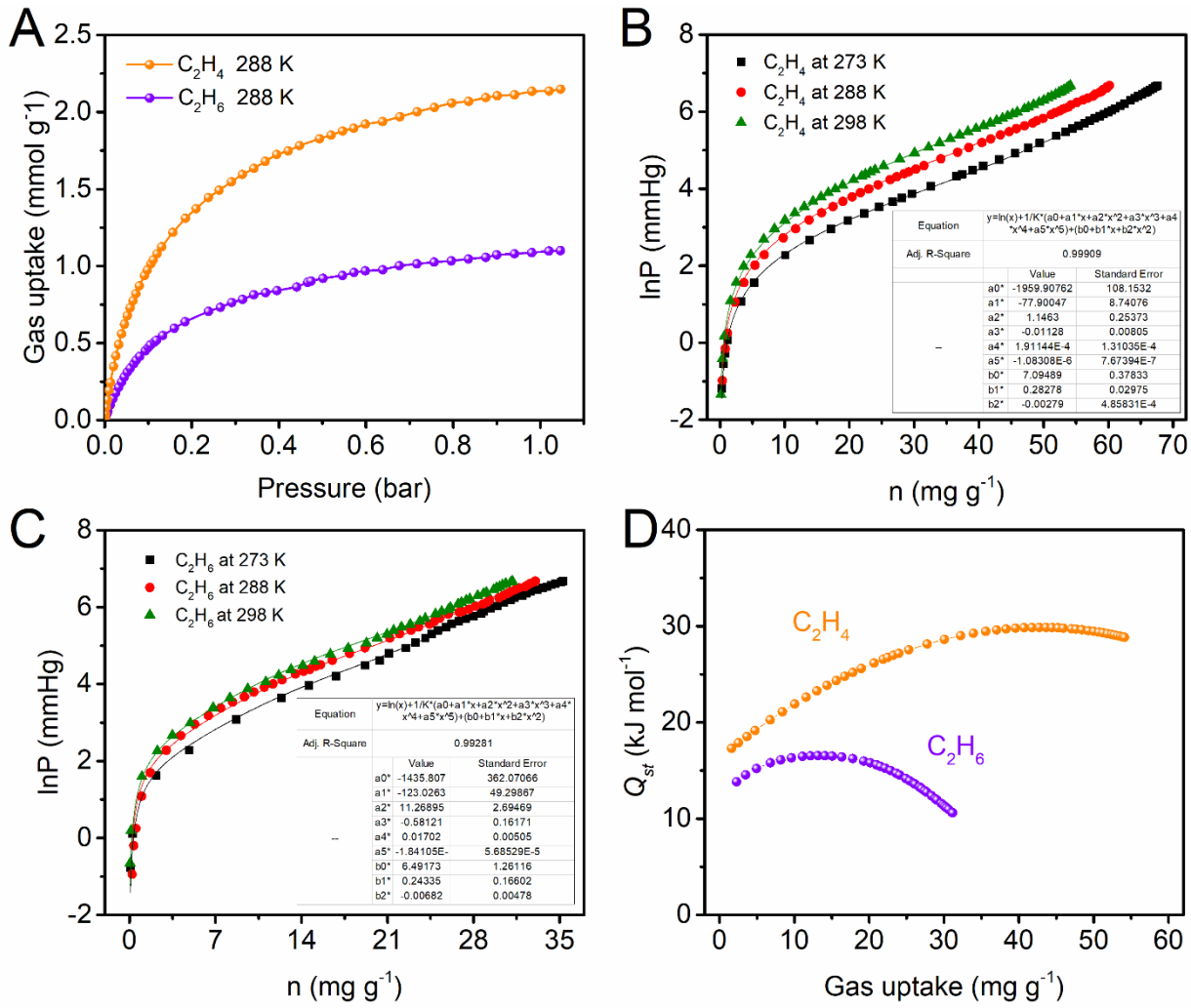


**Figure S2**. Virial fit of $C_2H_4$/$C_2H_6$ isotherms and the calculated isosteric heat of adsorption. (A) Adsorption isotherms of $ZnAtzPO_4$ for $C_2H_4$ and $C_2H_6$ at 288 K. (B)Virial fit of $C_2H_4$ isotherms at 273 K, 288 K and 298 K. (C) Virial fit of $C_2H_6$ isotherms at 273 K, 288 K and 298 K. (B) Isosteric heat of adsorption calculated for $C_2H_4$ and $C_2H_6$ on $ZnAtzPO_4$.

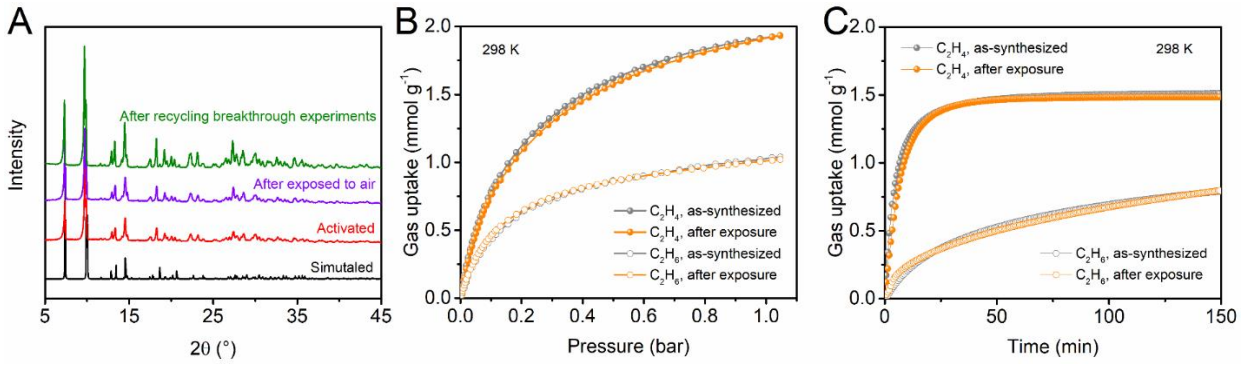


**Figure S3.** PXRD patterns, adsorption isotherms and time-dependent gas uptakes of as-synthesized $ZnAtzPO_4$ and samples after different treatments. (A) Simulated and experimental PXRD patterns of $ZnAtzPO_4$. (B) $C_2H_4/C_2H_6$ adsorption isotherms of as-synthesized $ZnAtzPO_4$ and sample after exposed to air (298 K, 70% humidity) for four weeks. (C) Time-dependent gas uptake profiles of as-synthesized $ZnAtzPO_4$ and sample after exposure treatment.

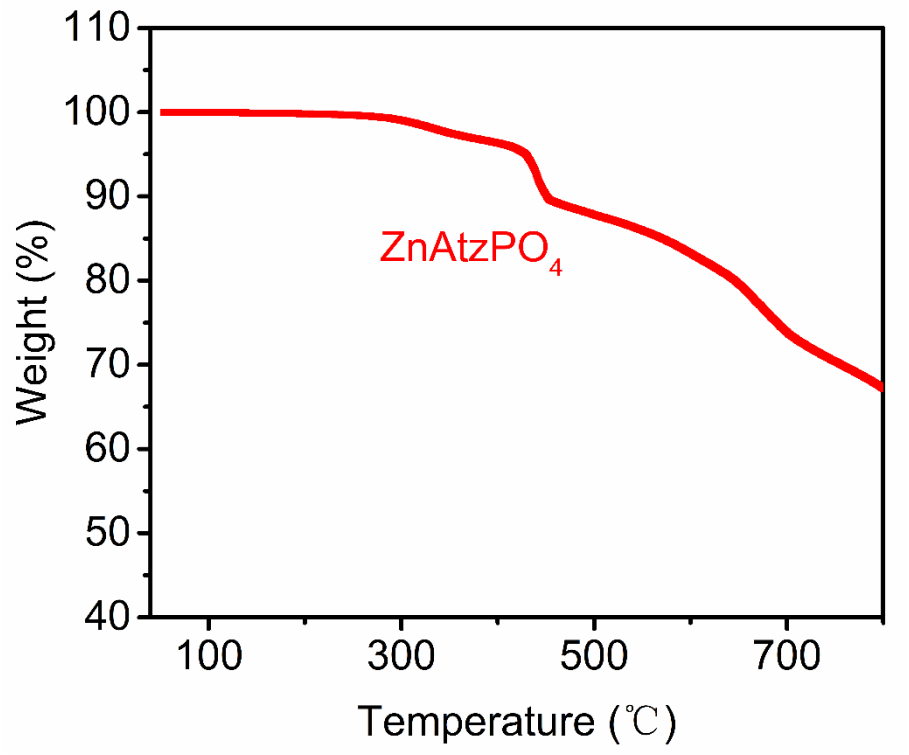


**Figure S4.** TGA curve of $ZnAtzPO_4$.

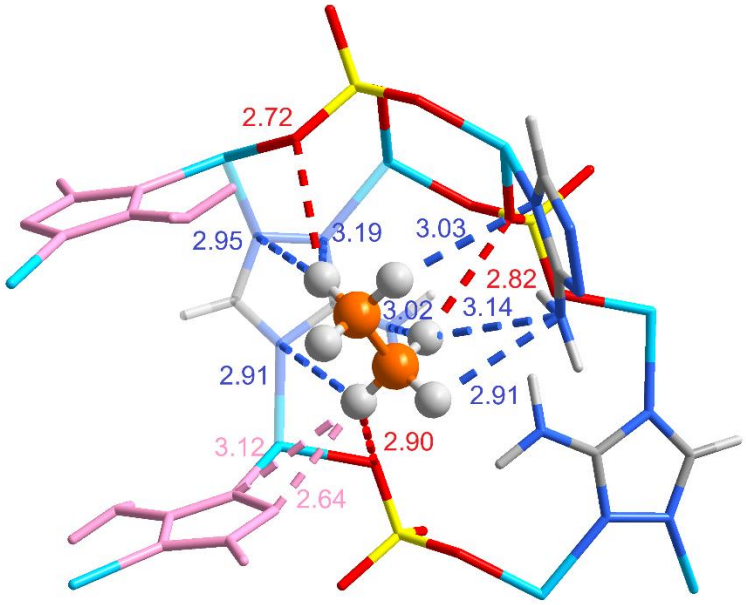


**Figure S5**. DFT-D calculated binding site of $C_2H_6$ in $ZnAtzPO_4$. (Color mode: C, gray-40%; H, gray-25%; N, light blue; Zn, sky blue; P, yellow; O, red. Bidentate coordinated Atz ligands are highlighted by rose. Broken lines refer to C-H…N/O hydrogen bonds. All interatomic distances are in angstroms.)

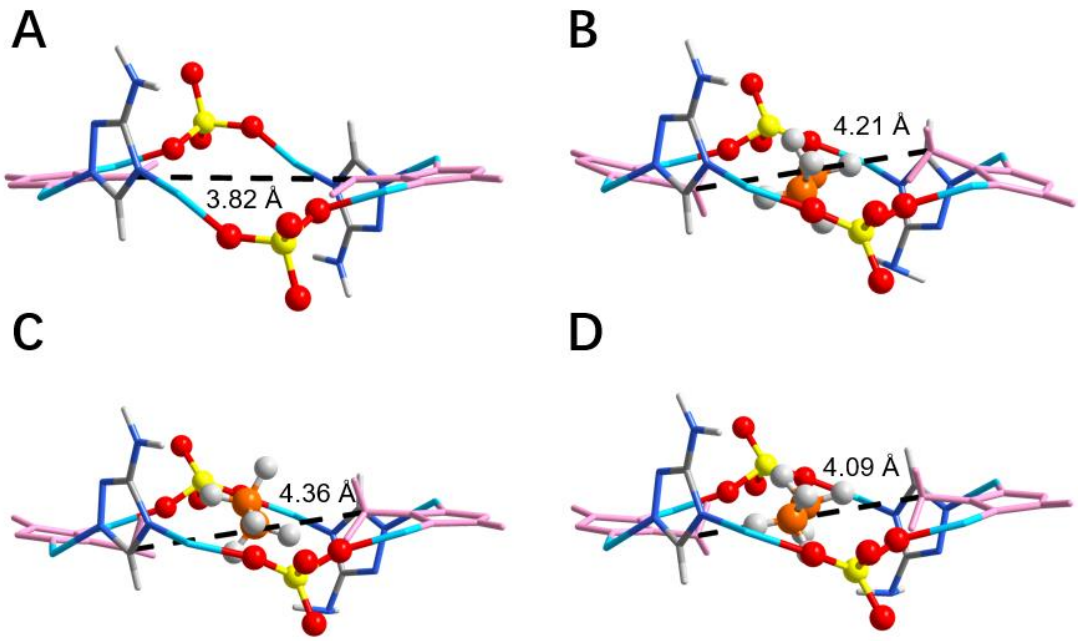


**Figure S6**. MD simulated snapshots of the bottleneck structure with and without $C_2H_6$ gas molecules. (A) Empty bottleneck structure without guest molecules. (B-D) Structures of the bottleneck with $C_2H_6$

molecule. (Color mode: C, gray-40%; H, gray-25%; N, light blue; Zn, sky blue. P, yellow; O, red. Bidentate coordinated Atz ligands are highlighted by rose.)

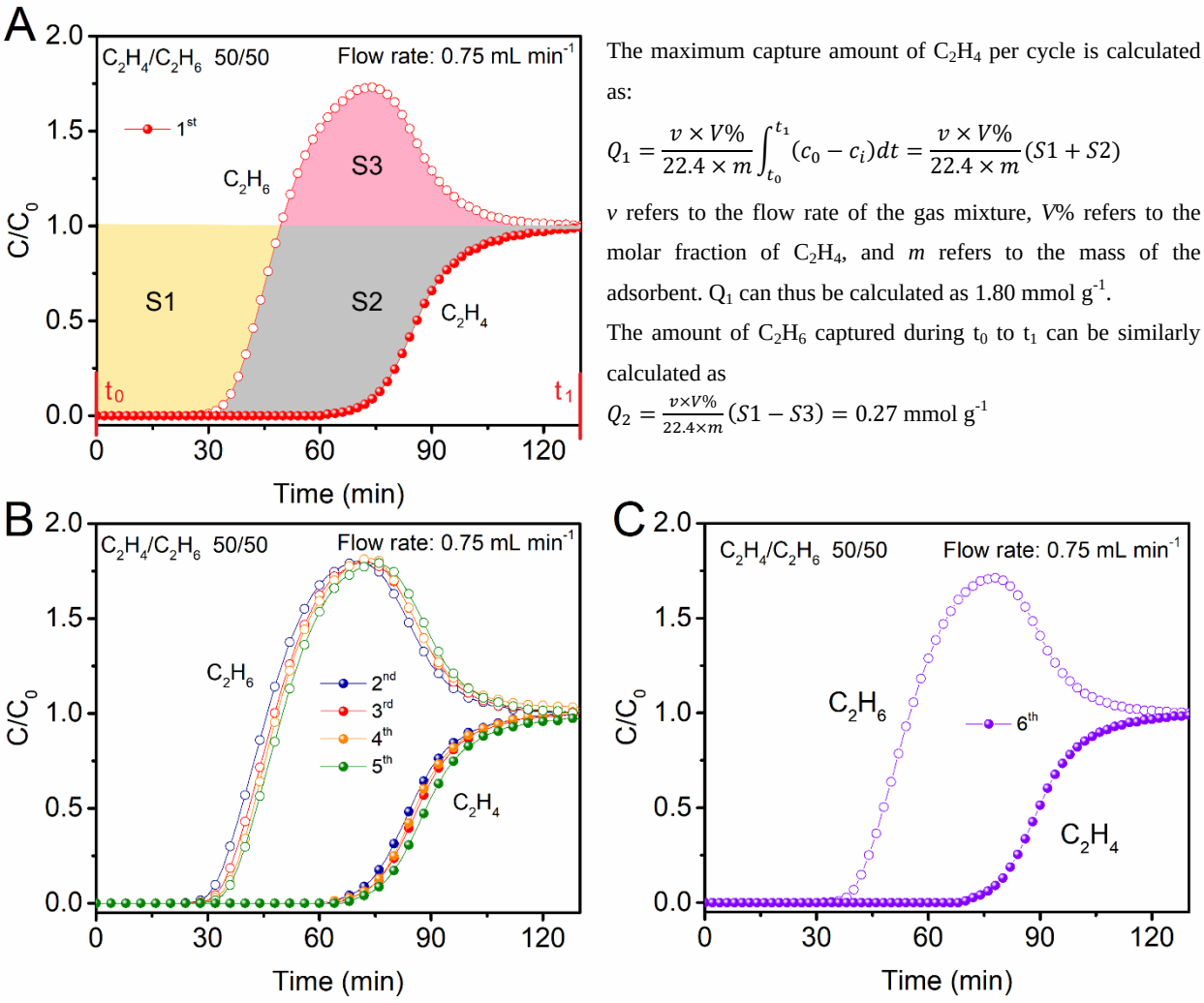


The maximum capture amount of $C_2H_4$ per cycle is calculated as:

$$Q_1 = \frac{v \times V\%}{22.4 \times m}\int_{t_0}^{t_1}(c_0 - c_i)dt = \frac{v \times V\%}{22.4 \times m}(S1 + S2)$$

$v$ refers to the flow rate of the gas mixture, $V\%$ refers to the molar fraction of $C_2H_4$, and $m$ refers to the mass of the adsorbent. $Q_1$ can thus be calculated as 1.80 mmol $g^{-1}$.

The amount of $C_2H_6$ captured during $t_0$ to $t_1$ can be similarly calculated as

$$Q_2 = \frac{v \times V\%}{22.4 \times m}(S1 - S3) = 0.27 \text{ mmol g}^{-1}$$

**Figure S7.** Recycling breakthrough experiments for $C_2H_4/C_2H_6$ (50:50, v/v) separation on $ZnAtzPO_4$ at 273 K and 1bar. The adsorption column was regenerated by heating to 373 K overnight between cycle in (A-B) and purging with He for 10 h in (C).

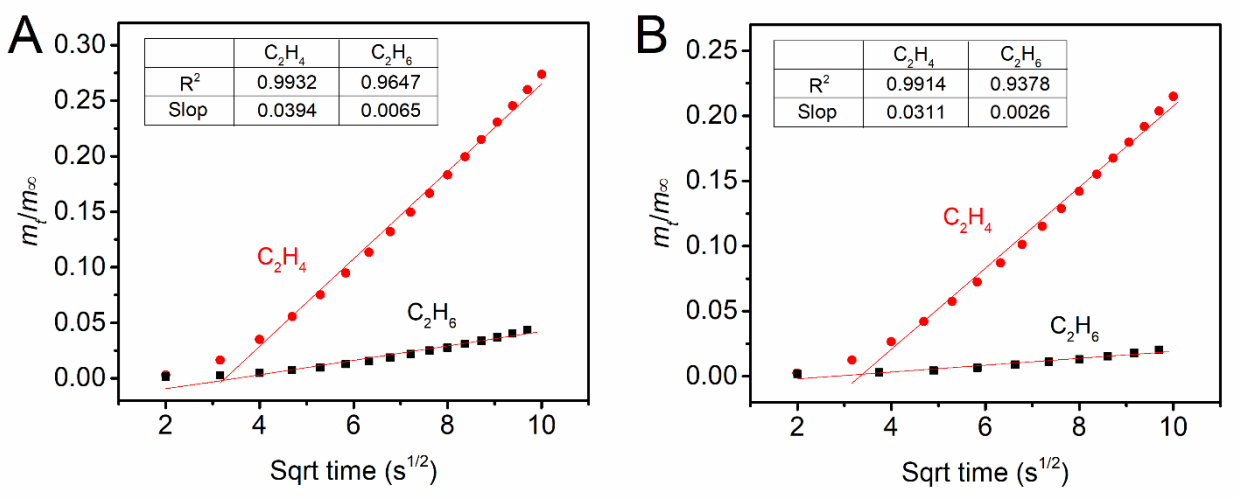


**Figure S8.** Fitting of diffusion time constants based on time-dependent gas uptake profiles of $C_2H_4$ and $C_2H_6$. (A-B) Fitting from data collected at 298 K (A) and 273 K (B).

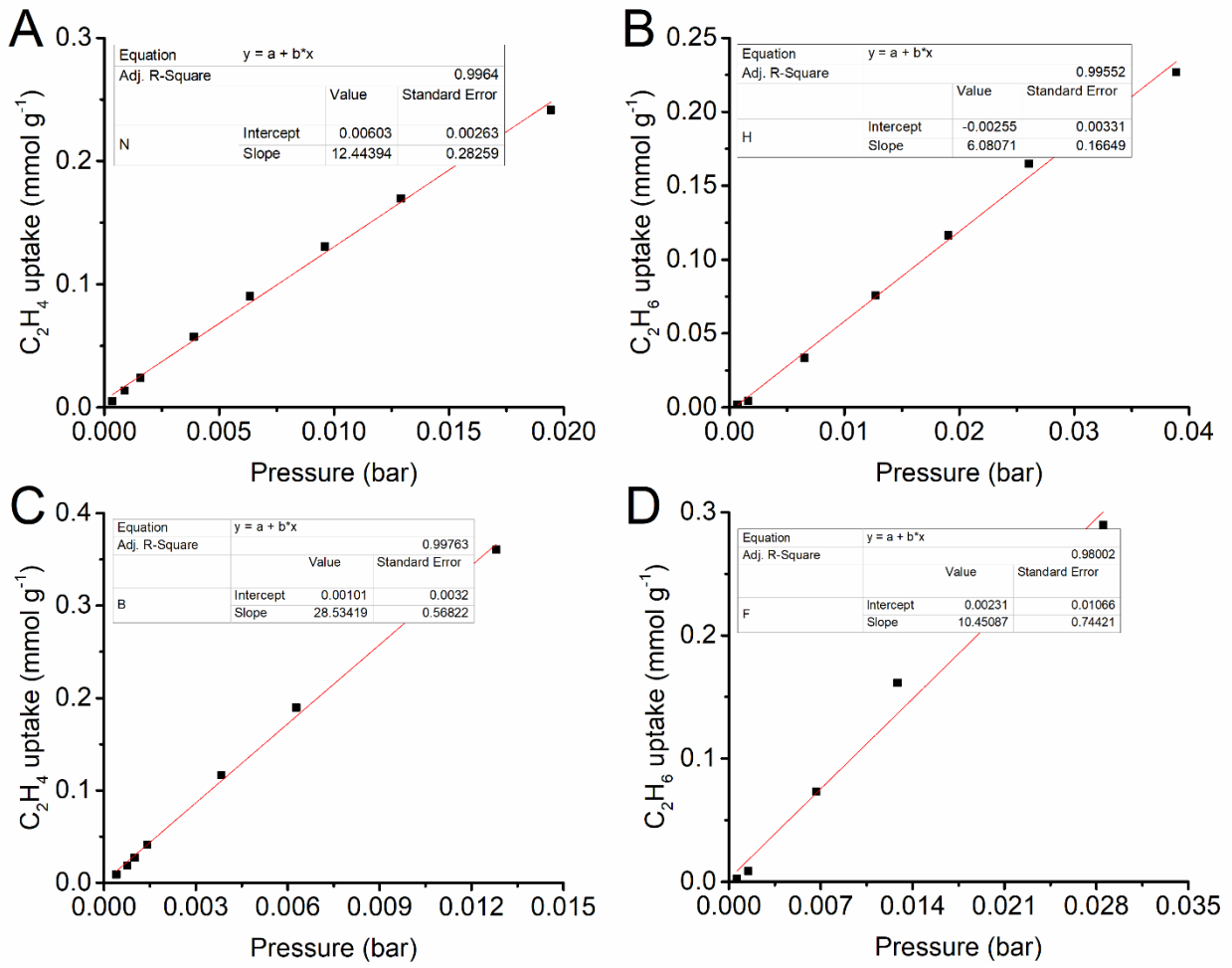


**Figure S9.** Fitting of Henry's constants based on adsorption isotherms of $C_2H_4$ and $C_2H_6$. (A) Fitting for

$C_2H_4$ at 298 K. (B) Fitting for $C_2H_6$ at 298 K. (C) Fitting for $C_2H_4$ at 273 K. (D) Fitting for $C_2H_6$ at 273 K.

**Table S1**. Comparison of $C_2H_4/C_2H_6$ adsorption properties of different porous materials.

| | $C_2H_4$ uptake (mmol $g^{-1}$)[a] | Volumetric $C_2H_4$ uptake (mmol $cm^{-3}$)[a] | $C_2H_6$ uptake (mmol $g^{-1}$)[a] | Uptake ratio ($C_2H_4/C_2H_6$)[a] | Kinetic selectivity ($C_2H_4/C_2H_6$) | Equilibrium-kinetic combined selectivity ($C_2H_4/C_2H_6$) | $Q_{st}$ for $C_2H_4$ (kJ $mol^{-1}$)[b] | $T$ (K) | Reference |
|---|---|---|---|---|---|---|---|---|---|
| $ZnAtzPO_4$ | 2.41 | 3.81 | 1.18 | 2.04 | 140.66 | 32.38 | 29.98 | 273 | This work |
| $ZnAtzPO_4$ | 1.92 | 3.04 | 1.04 | 1.85 | 36.59 | 12.40 | | 298 | |
| ITQ-55[c] | 1.5 | / | 1.77 | 0.85 | 90 | 6.36 | / | 303 | (*31*) |
| ITQ-29 | 1.66 | 2.36[d] | 1.68 | 0.99 | 1.02 | 1.33 | / | 301 | (*32*) |
| Si-CHA | 2.01 | / | 2.21 | 0.91 | 6.46 | 1.30 | / | 301 | (*32*) |
| Zeolite 5A | 2.45 | 2.84[d] | 1.72 | 1.42 | / | / | 37 | 303 | (*36*) |
| Fe-MOF-74 | 6.1 | 6.87 | 5.0 | 1.22 | / | / | 47.5 | 318 | (*20*) |
| HKUST-1 | 7.20 | 6.33 | 6.03 | 1.19 | / | / | 39 | 303 | (*35*) |
| PAF-1-$SO_3Ag$ | 4.06 | / | 2.23 | 1.82 | / | / | 106 | 296 | (*5*) |
| (Cr)-MIL-101-$SO_3Ag$ | 2.61 | / | 1.22 | 2.13 | / | / | 120 | 303 | (*21*) |
| UTSA-280 | 2.5 | 3.93 | 0.098 | 25.51 | / | / | 35.0 | 298 | (*24*) |
| Co-gallate | 3.37 | 5.18 | 0.31 | 10.87 | / | / | 44 | 298 | (*3*) |

[a] Gas uptakes and uptake ratios at 1 bar;

[b] Highest $Q_{st}$ values at different surface coverage;

[c] $C_2H_6$ uptakes were derived from GCMC simulations;

[d] Volumetric uptakes calculated based on particle densities.